

Hexadecapole strength in the region of the low-energy octupole resonance

Y. Fujita

College of General Education, Osaka University, Toyonaka, Osaka 560, Japan

M. Fujiwara, S. Morinobu, I. Katayama, T. Yamazaki, T. Itahashi, and H. Ikegami

Research Center for Nuclear Physics, Osaka University, Ibaraki, Osaka 567, Japan

S. I. Hayakawa

Ashikaga Institute of Technology, Ashikaga 326, Japan

(Received 22 June 1989)

The strength distributions of hexadecapole transitions have been measured for the closed-shell nuclei of ^{48}Ca , ^{50}Ti , ^{52}Cr , ^{54}Fe , ^{58}Ni , ^{90}Zr , and ^{208}Pb by using (p,p') reactions at $E_p = 65$ MeV. The peak-by-peak analysis revealed the distribution for the excitation energy up to around 10 MeV. In ^{208}Pb , the strength is distributed into two groups. One is the well-known first 4^+ state which exhausts an energy-weighted sum-rule fraction of 8.4%. The other is a bump consisting of clustering $L = 4$ states with a total fraction of 11.2%. The structure of the bump is much the same as those of low-energy octupole resonance, suggesting the existence of a resonance-like structure of hexadecapole strength. In an analysis using cumulative sum of the strength, a bump of a similar kind is recognized in each nucleus examined. These bumps exhaust 3–11% of the $E4$ energy-weighted sum rule and the centroids are situated at $E_x = 4$ –9 MeV.

I. INTRODUCTION

The isoscalar electric transitions are fundamental excitation modes in nuclei. The main parts of the $L = 0$ and 2 strengths have been observed in giant monopole resonance and in giant quadrupole resonance (GQR), respectively, and the $L = 3$ strength has been observed in low-energy and high-energy octupole resonances. The experimental information on the location and the distribution of the $L = 4$ strength, however, is so far rather scarce.¹ The harmonic-oscillator shell-model predicts three fundamental modes for the $L = 4$ vibration at energies of $0\hbar\omega$, $2\hbar\omega$, and $4\hbar\omega$ excitation. Almost no evidence has been reported for the presence of $4\hbar\omega$ isoscalar hexadecapole giant resonance which is predicted around $E_x \sim 150 A^{-1/3}$ MeV.¹ A small amount of $2\hbar\omega$ hexadecapole strength has been reported in the GQR region of ^{208}Pb and of Sn and Zr isotopes mainly through the evidence that the angular distribution of the GQR can be better fitted by including $L = 4$ strength.^{1–3} Therefore, the only well-known hexadecapole strength is the “fairly collective” low-lying $J^\pi = 4^+$ states at excitation energies of a few MeV. Usually, however, these states do not exhaust the whole $0\hbar\omega$ strength. For example, a theoretical calculation using random-phase approximation (RPA) predicts an energy-weighted sum-rule (EWSR) fraction of 13% in the $0\hbar\omega$ region of ^{208}Pb ,⁴ while the low-lying collective state at $E_x = 4.3$ MeV can account for about half of the strength.⁵

It should be noted, however, that RPA calculations predict that the isoscalar hexadecapole strength is fragmented over a wide energy range.^{4,6,7} In fact our high-resolution (p,p') data on ^{90}Zr indicated that many $L = 4$ states existed in the energy region of the low-energy octupole resonance (LEOR), i.e., $E_x = 5$ –8 MeV, in addition

to the well-known low-lying 4^+ states.⁸

In view of these theoretical and experimental circumstances, we thought it interesting to investigate the distribution of the hexadecapole strength in the LEOR region for various nuclei by high-resolution proton scattering. High resolution was very important in the experiment because $L = 4$ levels had to be separated from prevailing $L = 3$ levels, which formed as a whole a giant-resonance-like structure called LEOR.^{9–12}

II. EXPERIMENTAL PROCEDURE AND DATA ANALYSIS

A 65-MeV proton beam provided from the isochronous cyclotron at the Research Center for Nuclear Physics (RCNP), Osaka University, was used to bombard isotopically enriched target foils of ^{48}Ca , ^{50}Ti , ^{52}Cr , ^{54}Fe , ^{58}Ni , ^{90}Zr , and ^{208}Pb with 0.5–1.0 mg/cm² thickness. Inelastically scattered protons were analyzed by using a magnetic spectrograph RAIDEN,¹³ and were detected by a two-dimensional position-sensitive proportional counter system.¹⁴ Kinematic line broadening was compensated in order to attain high resolution.^{13–15} The overall resolutions of 10–22 keV were achieved in the present (p,p') experiments. As shown in Fig. 1 for the case of ^{208}Pb , a large number of levels were observed in each nucleus (see Ref. 11 for ^{48}Ca , Ref. 10 for ^{50}Ti , ^{52}Cr , and ^{54}Fe , Ref. 12 for ^{58}Ni , and Ref. 8 for ^{90}Zr). The width of each level was not noticeably wider than the instrumental one, indicating that the decay width was not as large. This is consistent with the fact that particle decay is prohibited, or at least hindered, in the so-called “LEOR region” examined here. Also noticeable is the fact that the continuous background, which was usually subtracted in the analysis of the LEOR, was not as high as those observed in the

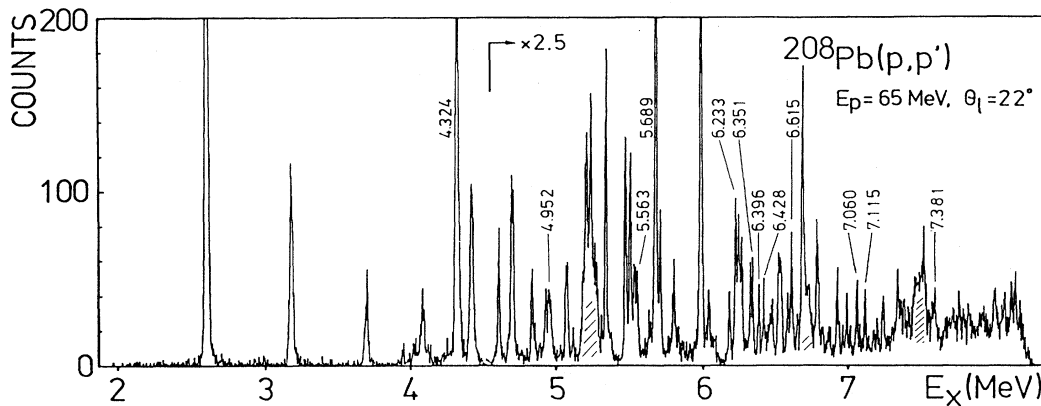


FIG. 1. Spectrum of inelastically scattered protons on the ^{208}Pb target at an angle near the maximum for the $L=4$ angular distribution. Prominent $L=4$ states are indicated by the excitation energy (in MeV). Broad peaks corresponding to contaminating light nuclei are shadowed.

measurements with lower-energy resolution. Spectra were analyzed by using a peak deconvolution program. The angular distributions were obtained in a wide range of angles for the states up to $E_x=13.6$ MeV for ^{48}Ca , 10.5 MeV for ^{50}Ti and ^{54}Fe , 9.5 MeV for ^{52}Cr , 12.0 MeV for ^{58}Ni , 8.6 MeV for ^{90}Zr , and up to 7.5 MeV for ^{208}Pb . Typical angular distributions for the states in the “LEOR region” are shown in Fig. 2 for ^{48}Ca and ^{208}Pb , the lightest and the heaviest target nuclei investigated here. The

angular distributions for the states with different L transfers peak at considerably different angles, showing a good selectivity to momentum transfer.

For each nucleus the angular distributions were analyzed with a distorted-wave Born-approximation (DWBA) code (Ref. 16) using a collective-model form factor and optical-potential parameters from Ref. 17. Angular distributions of 11–32 levels were in agreement with the $L=4$ DWBA calculations in the nuclei studied here. Details of the fit are found in Refs. 8–12. Inelastic proton scattering can excite isovector states or unnatural parity 3^+ and 5^+ states by $L=4$ transfer, and the observed $L=4$ states may be such states. In order to exclude the above possibilities, we compared the (p,p') and (α,α') spectra of ^{48}Ca . As a result, all the strong $L=4$ states have also been observed in an (α,α') experiment.¹¹ The situation was similar in ^{90}Zr .⁸ Thus, we believe that the contribution from isovector or unnatural-parity states is rather small.

The deformation length $\beta_L R$ was obtained for every state by comparing the data with the results of the DWBA calculation. The $E4$ EWSR percentage was derived by using the procedure given in Ref. 18. The obtained $\beta_L R$ values and EWSR fractions are summarized in Tables I–VI (for ^{58}Ni see Ref. 12). The distributions of strengths are shown in Fig. 3(a). As described in previous papers,^{9–12} many $L=3$ states have been observed in the energy region in which we search for $L=4$ states. As an example, the observed $L=3$ states of ^{208}Pb taken from Ref. 9 are also listed in Table VI.

III. DISCUSSION AND ANALYSIS

A. Hexadecapole strength

In order to see the validity of the $L=4$ strength obtained in this experiment, the deformation lengths for the low-lying states were compared with the values compiled in Nuclear Data Sheets. Generally they were in agreement within 20% for the nuclei examined here.

A common feature of the $E4$ strength distribution is its large fragmentation into many states with an EWSR frac-

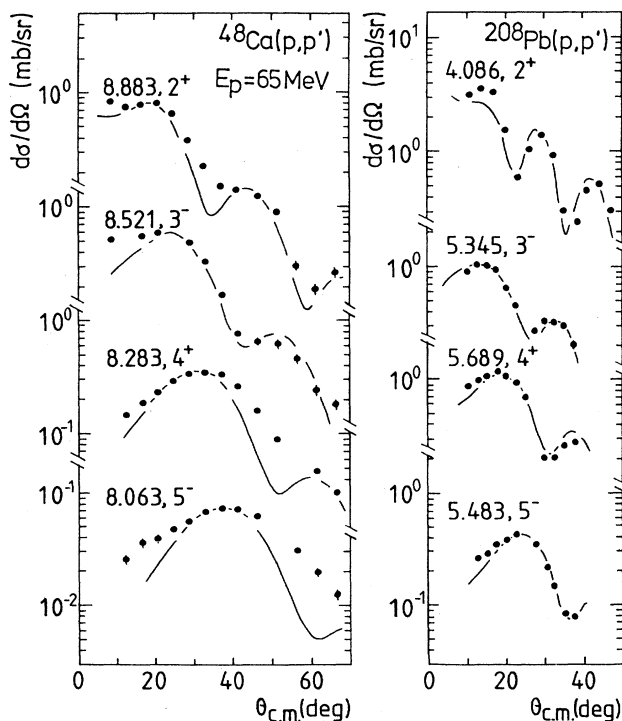


FIG. 2. Typical angular distributions for $J^\pi=2^+$, 3^- , 4^+ , and 5^- states in ^{48}Ca and ^{208}Pb in the energy region of LEOR. The DWBA calculations shown by the solid lines are normalized to the data.

TABLE I. Deformation lengths (βR) and EWSR percentages (S) for the $J^\pi=4^+$ states in ^{48}Ca .

E_x (MeV)	βR (fm)	S (%)	E_x	βR	S
6.345	0.32	1.00	10.065	0.07	0.07
6.648	0.24	0.60	10.107	0.12	0.21
7.469	0.11	0.13	10.399	0.07	0.07
7.800	0.19	0.41	10.586	0.08	0.09
7.956	0.08	0.08	10.955	0.12	0.26
8.178	0.05	0.03	11.050	0.07	0.09
8.248	0.21	0.58	11.098	0.09	0.14
8.283	0.25	0.79	11.125	0.06	0.05
8.471	0.07	0.07	11.248	0.09	0.14
8.797	0.21	0.60	11.622	0.09	0.13
9.158	0.08	0.08	12.162	0.08	0.12
9.621	0.13	0.27	12.271	0.10	0.20
9.784	0.07	0.08	12.369	0.06	0.07
9.992	0.09	0.13			

tion of typically 0.2–0.5 %, as seen from Fig. 3(a). It may be possible that weakly excited states with an EWSR fraction of less than 0.05% could not be identified especially at a high-excitation region where the level density is high and the present resolution is still not always good enough. But we believe that these weak states will not significantly alter the shape of the strength distribution obtained here.

Except for some states at a higher-excitation region, most of these fragmented 4^+ states are thought to be of the $0\hbar\omega$ excitation. A rather high-excitation energy of these states, comparable with that of $1\hbar\omega$ excitation, can be attributed to the shell effect; the shell energy of a high-spin $j_>$ orbit is depressed by the spin-orbit coupling. For example, in ^{48}Ca three $0\hbar\omega$ one-particle one-hole (p - h) transitions of $\nu(f_{7/2} \rightarrow 2p_{3/2})$, $\nu(f_{7/2} \rightarrow 2p_{1/2})$, and $\nu(f_{7/2} \rightarrow f_{5/2})$ can form 4^+ states around $E_x = 5$ –9 MeV. All of these transitions originate from the $\nu f_{7/2}$ orbit intruding into the lower bunch of the shell. A similar situation is true in ^{90}Zr , where four transitions of $\nu(g_{9/2} \rightarrow 2d_{5/2})$, $\nu(g_{9/2} \rightarrow 3s_{1/2})$, $\nu(g_{9/2} \rightarrow g_{7/2})$, and $\nu(g_{9/2} \rightarrow 2d_{3/2})$ are the candidates to form 4^+ states. The heavier the nucleus, the larger the number of candidates. In ^{208}Pb , there are five $0\hbar\omega$ p - h configurations which can form 4^+ states and have single p - h energies less than 7 MeV. They are $\pi(h_{11/2} \rightarrow h_{9/2})$, $\pi(h_{11/2} \rightarrow 2f_{7/2})$,

$\nu(i_{13/2} \rightarrow 2g_{9/2})$, $\nu(i_{13/2} \rightarrow i_{11/2})$, and $\nu(i_{13/2} \rightarrow 3d_{5/2})$. In addition to these, two transitions $\pi(2d_{5/2} \rightarrow i_{13/2})$ and $\nu(2f_{7/2} \rightarrow j_{15/2})$, which are originally categorized as $2\hbar\omega$ transitions, have a rather small single p - h energy of about 7.3 MeV. It is reasonable to think that these seven configurations mainly contribute to the observed strength in ^{208}Pb .

The sum of the EWSR percentages of the hexadecapole strength is small in light nuclei (4–6 %) and larger in heavier nuclei, as summarized in Table VII. Particularly in ^{208}Pb , as much as 20.2% has been observed. The enhancement in ^{208}Pb may partly be explained by the contribution of the $2\hbar\omega$ excitations mentioned above. However, considering that this value is even larger by about 50% than the result of the RPA calculation,⁴ we can note a rather high collectivity of the hexadecapole strength in the “ $0\hbar\omega$ region” of ^{208}Pb . It is interesting that the EWSR percentage of 20% is nearly comparable to or larger than the component of 8–29 % found in the GQR region.^{2,3} This fact shows that a significant part of the strength is localized in the “ $0\hbar\omega$ region” in ^{208}Pb in spite of the belief that the hexadecapole strength is almost evenly divided into the $2\hbar\omega$ and $4\hbar\omega$ regions.⁴ It is also of interest to compare this result to that for the octupole strength in ^{208}Pb , where as much as 35% of the EWSR has been found in the $1\hbar\omega$ region, while in lighter

TABLE II. Deformation lengths (βR) and EWSR percentages (S) for the $J^\pi=4^+$ states in ^{50}Ti .

E_x (MeV)	βR (fm)	S (%)	E_x	βR	S
2.675	0.40	0.71	6.476	0.09	0.16
4.147	0.19	0.24	6.519	0.31	1.02
5.378	0.21	0.38	6.709	0.23	0.55
5.433	0.08	0.06	8.035	0.13	0.21
5.787	0.23	0.48	9.391	0.11	0.17
5.817	0.17	0.27			

TABLE III. Deformation lengths (βR) and EWSR percentages (S) for the $J^\pi=4^+$ states in ^{52}Cr .

E_x (MeV)	βR (fm)	S (%)	E_x	βR	S
2.369	0.33	0.43	5.425	0.32	0.96
2.768	0.30	0.41	5.541	0.07	0.05
3.415	0.13	0.10	7.140	0.14	0.23
4.040	0.16	0.18	7.278	0.13	0.22
4.630	0.36	0.98	7.848	0.11	0.15
5.095	0.15	0.19	7.893	0.12	0.18

nuclei at most 25% has been observed.⁹

Considering the limited number of 1p-1h configurations which can form 4^+ states in the energy region we examined, spreading of the 1p-1h strengths into highly structured states, probably of 2p-2h nature, is also an interesting subject. The observation of the fragmentation would hopefully offer an important clue for the theoretical investigation on the damping mechanism of a nuclear excitation.¹⁹

B. Bump structure in the region of LEOR

From the upper part of Fig. 4(a), it is seen that the hexadecapole strength in ^{208}Pb is divided into two groups, i.e., the low-lying collective state and a bump consisting of many states clustering around $E_x=6$ MeV. This feature reminds us of the $L=3$ strength, which is shown in the lower part of Fig. 4(a); the strength is distributed into a low-lying collective state and many clustering states which form as a whole a giant-resonance-like structure, i.e., the LEOR.⁹ It is clear that both the $L=3$ and 4 strength distributions in ^{208}Pb are quite similar in their structure, though the separation between the low-lying state and the bump is somewhat different; it is smaller in the $L=4$ distribution than in the $L=3$ distribution. In order to study the strength distribution as a function of excitation energy, the cumulative sums of the $L=3$ and 4 strengths are plotted in Fig. 4(b). The ordinate gives the EWSR percentage divided by the excitation energy in order to eliminate the weight by energy and to show the strength proportional to the single-particle strength of a state.²⁰ In this figure the cumulative sum of the $L=3$ strength shows the first rise corresponding to the first 3^- state. The LEOR is characterized by a shape like a

“stretched S ” characteristic of a resonance structure. We can see almost the same structure for the $L=4$ cumulative sum.

In the harmonic-oscillator shell-model picture, the $L=2$ strength is located at excitation energies of $0\hbar\omega$ and $2\hbar\omega$, and the $L=3$ strength at $1\hbar\omega$ and $3\hbar\omega$. The $0\hbar\omega$, $L=2$ strength is concentrated in one, or at most, a small number of low-lying $J^\pi=2^+$ states, while the $1\hbar\omega$, $L=3$ strength is distributed into one or a few collective low-lying states and the bump called LEOR which have been systematically observed at $E_x \sim 30A^{-1/3}$ MeV.¹ It seems that the distribution of strength becomes wider as L becomes larger. It is therefore not strange that the $0\hbar\omega$, $L=4$ strength is also distributed among the low-lying state(s) and a cluster of states which constitute a bump at a somewhat higher-excitation energy, as we have seen in the case of ^{208}Pb .

The above point of view is supported by the observed hexadecapole strength in ^{48}Ca , ^{50}Ti , and ^{58}Ni shown in Fig. 3(a); in these nuclei the strengths are categorized into two groups, i.e., a low-lying state (in ^{48}Ca two low-lying states) and a bump at a higher excitation. However, this feature is not as clear as in ^{208}Pb . In the lighter nuclei, the configuration space to form 4^+ states is rather limited, as we discussed earlier, and the $L=4$ strength distribution is affected by shell effects. The effects are clearly seen in the case of ^{48}Ca , a doubly closed-shell nucleus. The first 4^+ state in ^{48}Ca appears above 6 MeV of excitation which is about 4 MeV higher than that in the other $f_{7/2}$ nuclei. The distribution for ^{90}Zr is starting to look similar to the one for ^{208}Pb in gross feature. It may seem rather difficult to find common features of the 4^+ states among the nuclei examined here, but the cumulative sums which show more clearly the strength distribution

TABLE IV. Deformation lengths (βR) and EWSR percentages (S) for the $J^\pi=4^+$ states in ^{54}Fe .

E_x (MeV)	βR (fm)	S (%)	E_x	βR	S
2.538	0.31	0.43	5.703	0.14	0.20
3.295	0.22	0.28	6.484	0.15	0.26
3.834	0.37	0.93	6.607	0.11	0.13
4.048	0.14	0.13	6.670	0.11	0.14
4.265	0.31	0.72	6.881	0.11	0.14
4.949	0.16	0.21	7.674	0.09	0.11
5.232	0.14	0.19	8.666	0.13	0.24
5.657	0.12	0.15	10.342	0.09	0.15

TABLE V. Deformation lengths (βR) and EWSR percentages (S) for the $J^\pi=4^+$ states in ^{90}Zr .

E_x (MeV)	βR (fm)	S (%)	E_x	βR	S
3.077	0.21	0.41	6.709	0.11	0.24
4.068	0.14	0.24	6.828	0.08	0.11
4.340	0.29	1.04	6.868	0.08	0.11
4.952	0.19	0.05	6.910	0.09	0.17
5.221	0.12	0.22	7.075	0.09	0.18
5.387	0.19	0.55	7.166	0.08	0.12
5.470	0.17	0.46	7.290	0.06	0.06
5.989	0.09	0.15	7.538	0.11	0.25
6.071	0.11	0.23	7.782	0.04	0.04
6.179	0.12	0.24	7.811	0.09	0.17
6.323	0.12	0.26	7.892	0.10	0.21
6.532	0.07	0.09	7.941	0.10	0.23
6.681	0.12	0.29	7.999	0.05	0.06

as a function of excitation energy reveal very interesting physical features. Strong peaks are observed around $E_x=4$ MeV in ^{54}Fe and ^{90}Zr , around $E_x=5$ MeV in ^{52}Cr and ^{58}Ni , around $E_x=6$ MeV in ^{50}Ti and ^{208}Pb , and around $E_x=8$ MeV in ^{48}Ca . Thus cumulative sums shown in Fig. 3(b) increase considerably around $E_x=4-8.5$ MeV, but not as much at a higher-excitation energy, and they show a stretched S shape. Then it may be concluded that the envelope of the $E4$ strength around $E_x=3-10$ MeV exhibits a resonance structure with a width of about 1 MeV. Here we would tentatively call the structure a low-energy hexadecapole resonance (LEHR) simply by the similarity of structure with the LEOR.

In ^{58}Ni , the spectra of which have been analyzed inten-

sively up to $E_x=12$ MeV, an increase of the cumulative sum has been observed above $E_x=9$ MeV. The EWSR fraction is 2.2% in total. It is natural to think that these strengths are the tail part of the $2\hbar\omega$ excitation, i.e., of the "giant" hexadecapole resonance which has been observed in ^{208}Pb .³ From this viewpoint, the increase of the sum above 9.5 MeV in ^{48}Ca may also be attributed to the $2\hbar\omega$ excitation. Actually many fragmented 2^+ states have been observed above $E_x=10.5$ MeV in ^{48}Ca ,¹¹ and they have been thought to be the lower tail of the GQR, which is naturally of $2\hbar\omega$ nature. According to this interpretation, 2.8 and 2.1% of the EWSR fraction in the resonance region of ^{48}Ca is subdivided into $0\hbar\omega$ and $2\hbar\omega$ regions, respectively.

In order to know the width Γ and the central value of

TABLE VI. Deformation lengths (βR) and EWSR percentages (S) for the $J^\pi=3^-$ and 4^+ states in ^{208}Pb .

E_x (MeV)	βR (fm)	S (%)	E_x	βR	S
Sum-rule fractions for $J^\pi=3^-$ states					
2.615	0.83	20.37	6.276	0.13	1.11
4.698	0.20	2.11	6.445	0.06	0.29
4.934	0.13	0.90	6.704	0.10	0.75
5.244	0.15	1.39	6.736	0.05	0.23
5.318	0.05	0.17	6.940	0.06	0.27
5.345	0.25	3.70	7.171	0.05	0.23
5.515	0.17	1.77	7.334	0.12	1.20
5.877	0.06	0.25	7.517	0.10	0.87
Sum-rule fractions for $J^\pi=4^+$ states					
4.324	0.54	8.41	6.233	0.16	1.03
4.952	0.09	0.30	6.351	0.10	0.41
5.563	0.11	0.44	6.396	0.11	0.54
5.689	0.29	3.30	6.428	0.10	0.44
5.774	0.06	0.13	6.615	0.14	0.90
5.796	0.06	0.13	7.060	0.11	0.56
5.813	0.14	0.78	7.115	0.10	0.47
6.009	0.13	0.69	7.381	0.10	0.49
6.052	0.12	0.54			

the excitation energy E_0 of the resonance structure, the cumulative strength sum was fitted to the integrated Breit-Wigner function

$$Y(E) = Y_0 \left[\frac{1}{2} + \pi^{-1} \tan^{-1} 2(E - E_0)/\Gamma \right], \quad (1)$$

where Y_0 is the integrated strength. The obtained values for E_0 and Γ are given in Table VII. The E_0 values vary from 4.2 MeV of ^{54}Fe to 8.7 (8.3) MeV of ^{48}Ca . The excitation energy E_0 of a GR is usually assumed to be proportional to $A^{-1/3}$. Thus the value $E_0 A^{1/3}$ is regarded to give an excitation energy irrelevant to the mass of a nucleus. The values for $E_0 A^{1/3}$ are given in Table VII and plotted in Fig. 5(a). It seems that the value is related with the shell structure, because the value decreases monotonously among $N=28$ nuclei from ^{48}Ca to ^{54}Fe in accordance with the addition of protons to the $Z=20$ proton shell closure. It may be of interest to compare the values of the LEHR with those of LEOR shown in Fig. 5(b), because the excitation energy and the structure of them are rather similar. In both Figs. 5(a) and 5(b), we notice larger values for doubly closed-shell nuclei ^{48}Ca , ^{90}Zr , and ^{208}Pb . We also notice a somewhat similar trend among $N=28$ nuclei, but the fluctuation is large in the LEHR, while in the LEOR the deviation from the mean value ($E_0 A^{1/3}=30$) is small. Thus, in spite of the resonance-like structure similar to the LEOR, the shell effects are much stronger in the lighter nuclei studied here and the LEHR in these nuclei behaves less like a GR which shows rather systematic behavior of the excitation energy as a function of mass number.

A small width Γ has been obtained for ^{48}Ca and ^{208}Pb while a large one has been obtained for ^{90}Zr . From a theory describing the width Γ of a GR, the width is proportional to E^2 .¹⁹ The value Γ/E^2 is supposed to give a good measure of the ‘‘intrinsic width’’ of a resonance structure. The obtained values are summarized in Table VII. The value is very small in both ^{48}Ca and ^{208}Pb , suggesting a rather high collectivity of the structure in these nuclei.

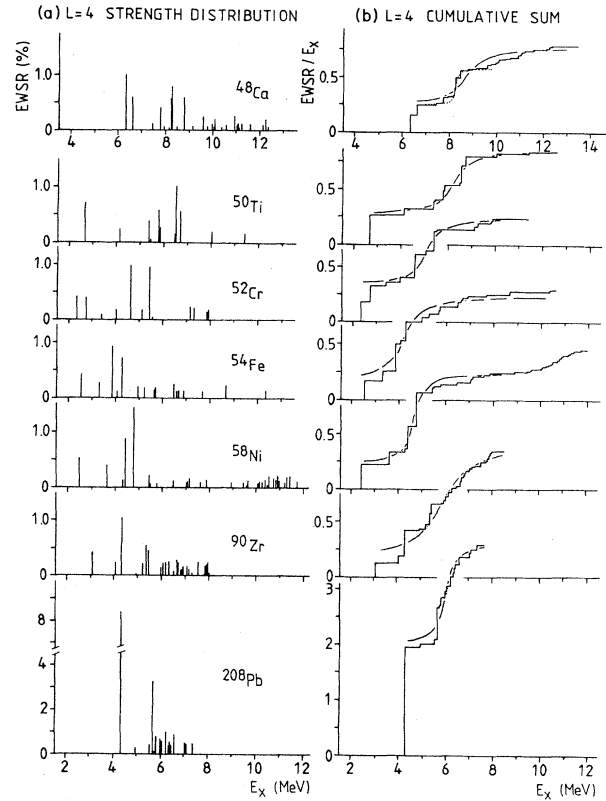


FIG. 3. (a) Strength distribution of $L=4$ states as a function of excitation energy. The strength is given by the percentage of EWSR. (b) Cumulative sum of the strengths. The ordinate gives the percentage of the EWSR divided by E_x (MeV), showing the strength proportional to single-particle strength. The analyses have been performed up to the excitation energies where the lines of cumulative sum terminate. Solid curved lines represent the fit of the cumulative sum to the ensemble strength function given by Eq. (1). The dotted curved line in the figure of ^{48}Ca is the result of the fit assuming that the $0\hbar\omega$ region is only up to $E_x=9.5$ MeV. For the detail, see the text.

TABLE VII. Observed properties of hexadecapole strengths.

	Low-lying 4^+			Resonance structure (LEHR)					Number of states
	E_x (MeV)	βR fm	EWSR (%)	E_0 (MeV)	$E_0 A^{1/3}$	EWSR (%)	Γ (MeV)	Γ/E^2	
^{48}Ca	6.35	0.32	1.0	8.7 ± 0.2^a	32 ^a	4.9 ^a	1.1 ± 0.3^a	0.015 ^a	25 ^a
	6.65	0.24	0.6	$(8.3 \pm 0.1)^b$	(30) ^b	(2.8) ^b	$(0.2 \pm 0.1)^b$	(0.002) ^b	(9) ^b
^{50}Ti	2.68	0.40	0.7	6.3 ± 0.2	23	3.5	1.0 ± 0.3	0.025	10
^{52}Cr	2.37	0.33	0.4	5.2 ± 0.2	19	3.2	0.8 ± 0.3	0.029	10
	2.77	0.30	0.4						
^{54}Fe	2.54	0.31	0.4	4.2 ± 0.2	16	3.8	1.0 ± 0.3	0.057	14
^{58}Ni	2.46	0.35	0.6	4.7 ± 0.1	18	4.0	0.6 ± 0.2	0.027	13
^{90}Zr	3.08	0.21	0.4	5.9 ± 0.2	26	5.8	1.8 ± 0.3	0.052	25
^{208}Pb	4.32	0.54	8.4	6.0 ± 0.2	36	11.2	0.6 ± 0.2	0.017	16

^aAssuming a wide distribution of LEHR shown by a solid curved line in Fig. 3(b).

^bAssuming a narrow distribution of LEHR shown by a dotted curved line in Fig. 3(b).

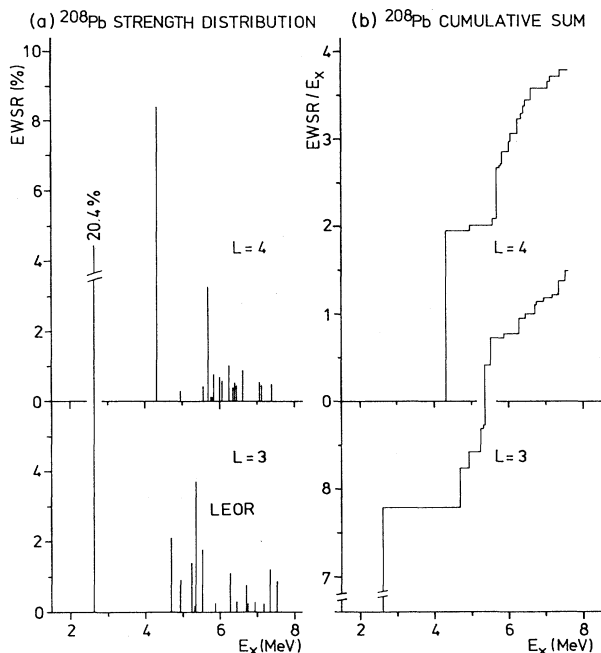


FIG. 4. (a) Distributions of the EWSR percentage for the $L=3$ and 4 strengths in ^{208}Pb . (b) Cumulative sum of the strengths. The ordinate gives the percentage of EWSR divided by E_x (MeV), showing the strength proportional to single-particle strength.

IV. SUMMARY AND CONCLUSION

Many $L=4$ states have been observed in various nuclei at $E_x=2-12$ MeV. Judging from the excitation energy, most of these states belong to the $0\hbar\omega$ excitation. The observed $L=4$ states could be categorized into two groups in each nucleus. They are the low-lying state(s) and a bump which consists of a cluster of states concentrating at higher energies than those of low-lying states. The structure of the bump is rather similar to that of the LEOR, and the envelope of the bump exhibits a resonance-like structure. We tentatively call this structure LEHR. The energy region of the LEHR is similar to that of the LEOR. The centroid of the LEHR, however, is more fluctuating from nucleus to nucleus than that of the LEOR. The exhaustion of the sum rule also generally increases with increasing mass number. From this point of view the LEHR behaves less like a usual GR, but somewhat like a low-lying state. It seems that the LEHR is affected more or less by the structure of individual nucleus. Recently, the LEOR of Ti isotopes have been studied systematically for ^{50}Ti , ^{48}Ti , and ^{46}Ti .²¹ The experiment has revealed that the centroid energy of the LEOR decreases as the neutron number deviates from $N=28$ shell closure. Especially in ^{46}Ti , it is found that the centroid energy decreases to about one-half of the value expected from systematics and the low-lying state cannot be distinguished from the LEOR anymore. This fact suggests that the excitation energy of a resonance-like struc-

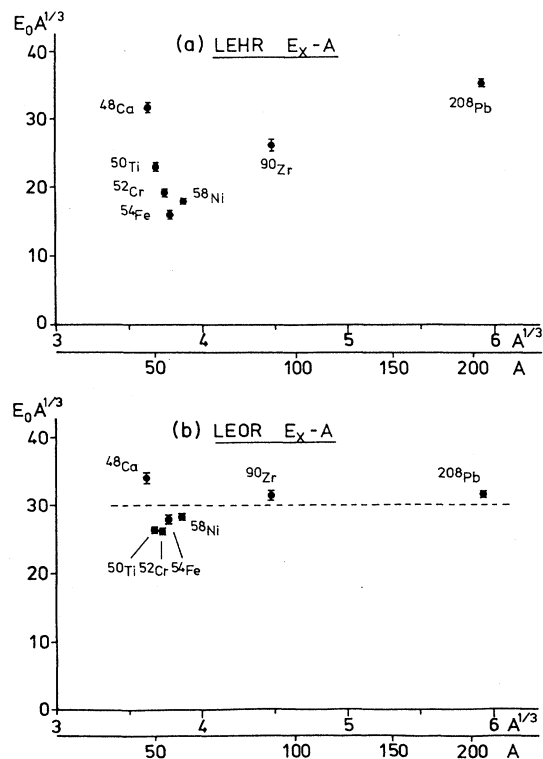


FIG. 5. (a) Normalized excitation energy $E_0 A^{1/3}$ of the LEHR as a function of mass number A . (b) Normalized excitation energy $E_0 A^{1/3}$ of the LEOR as a function of mass number A . The dotted line shows the mean value $E_0 A^{1/3}=30$. The $L=3$ strength distributions given in Refs. 8-12 have been used in order to obtain values of E_0 .

ture with higher L and low-excitation energy, like LEOR or LEHR, is rather sensitive to the individual nuclear structure such as shell closure or nuclear deformation. Another point which should be emphasized is that the resonance structure is prominent in ^{208}Pb , the heaviest nucleus examined here. This may reflect the suggestion that an excitation with a high- L multipole such as 4^+ would require a large nucleus to have its collective properties fully exhibited.⁶

Finally we would like to emphasize that bumps which have been thought simply to be the low-energy octupole resonance have structures; the bumps consist of octupole states and hexadecapole states. They have been separated through a peak-by-peak analysis of high-resolution spectra, contrary to the usual method of identifying a bump as a resonance structure.

ACKNOWLEDGMENTS

The authors are grateful to the cyclotron crew of the Research Center for Nuclear Physics (RCNP), Osaka University, for their kind support. Part of this work was performed at Giessen when one of the authors (Y.F.) was staying in the Federal Republic of Germany. He expresses his gratitude to Professor D. Fick (Universität

Marburg), Dr. V. Kitipova, and Professor K. T. Knöpfle (Max Planck Institut, Heidelberg) for valuable comments. He is grateful to Professor H. Wollnik (Universität Giessen) and Professor N. Takahashi (Osaka University)

for their encouragement and to the Alexander-von-Humboldt Foundation for its support. The experiment was performed at RCNP under Program Nos. 8A20, 9C01, 11A09, and 13A01.

-
- ¹F. E. Bertrand, Nucl. Phys. **A354**, 129 (1981); J. Speth and A. van der Woude, Rep. Prog. Phys. **44**, 719 (1981); A. van der Woude, Prog. Part. Nucl. Phys. **18**, 217 (1987); and references in these review papers.
- ²M. N. Harakeh, B. van Heyst, K. van der Borg, and A. van der Woude, Nucl. Phys. **A327**, 373 (1979); T. Yamagata, S. Kishimoto, K. Iwamoto, K. Yuasa, M. Tanaka, S. Nakayama, T. Fukuda, M. Inoue, M. Fujiwara, Y. Fujita, I. Miura, and H. Ogata, Phys. Lett. **123B**, 169 (1983).
- ³D. K. McDaniels, J. R. Tinsley, J. Lisantti, D. M. Drake, I. Bergqvist, L. W. Swenson, F. E. Bertrand, E. E. Gross, D. J. Horen, T. P. Sjoreen, R. Liljestrang, and H. Wilson, Phys. Rev. C **33**, 1943 (1986).
- ⁴K. F. Liu and G. E. Brown, Nucl. Phys. **A265**, 385 (1976).
- ⁵M. J. Martin, Nucl. Data Sheets **47**, 797 (1986).
- ⁶G. F. Bertsch and S. F. Tsi, Phys. Rep. **18**, 125 (1975).
- ⁷G. A. Rinker and J. Speth, Nucl. Phys. **A306**, 360 (1978).
- ⁸Y. Fujita, M. Fujiwara, S. Morinobu, I. Katayama, T. Yamazaki, T. Itahashi, H. Ikegami, and S. I. Hayakawa, Phys. Lett. **98B**, 175 (1981).
- ⁹Y. Fujita, M. Fujiwara, S. Morinobu, I. Katayama, T. Yamazaki, T. Itahashi, H. Ikegami, and S. I. Hayakawa, Phys. Rev. C **32**, 425 (1985).
- ¹⁰M. Fujiwara, Y. Fujita, S. Imanishi, S. Morinobu, T. Yamazaki, H. Ikegami, K. Katori, and S. I. Hayakawa, Phys. Rev. C **32**, 830 (1985).
- ¹¹Y. Fujita, M. Fujiwara, S. Morinobu, T. Yamazaki, T. Itahashi, H. Ikegami, and S. I. Hayakawa, Phys. Rev. C **37**, 45 (1988).
- ¹²M. Fujiwara, Y. Fujita, I. Katayama, S. Morinobu, T. Yamazaki, H. Ikegami, S. I. Hayakawa, and K. Katori, Phys. Rev. C **37**, 2885 (1988).
- ¹³H. Ikegami, S. Morinobu, I. Katayama, M. Fujiwara, and S. Yamabe, Nucl. Instrum. Methods **175**, 335 (1981).
- ¹⁴Y. Fujita, K. Nagayama, M. Fujiwara, S. Morinobu, T. Yamazaki, and H. Ikegami, Nucl. Instrum. Methods **217**, 441 (1983).
- ¹⁵Y. Fujita, S. Morinobu, M. Fujiwara, I. Katayama, T. Yamazaki, and H. Ikegami, Nucl. Instrum. Methods **225**, 298 (1984), and references therein.
- ¹⁶P. D. Kunz, DWUCK, a DWBA computer program, University of Colorado (unpublished).
- ¹⁷H. Sakaguchi, M. Nakamura, K. Hatanaka, A. Goto, T. Noro, F. Ohtani, H. Sakamoto, H. Ogawa, and S. Kobayashi, Phys. Rev. C **26**, 944 (1982).
- ¹⁸G. R. Satchler, Nucl. Phys. **A195**, 1 (1972).
- ¹⁹G. F. Bertsch, P. F. Bortignon, and R. A. Broglia, Rev. Mod. Phys. **55**, 287 (1983).
- ²⁰A. Bohr and B. R. Mottelson, *Nuclear Structure* (Benjamin, New York, 1969), Vol. 1, Chap. 2.
- ²¹A. Higashi, M. Fujiwara, S. I. Hayakawa, N. Ikeda, H. Ikegami, I. Katayama, K. Katori, H. Miyatake, S. Morinobu, and M. Tosaki, Phys. Rev. C **39**, 1286 (1989); M. Fujiwara, S. Morinobu, M. Tosaki, H. Ito, I. Katayama, H. Ikegami, S. I. Hayakawa, N. Ikeda, H. Ohsumi, A. Higashi, and K. Katori, *ibid.* **35**, 1257 (1987).